Airborne LIDAR data segmentation based on 3D mathematical morphology

WU Hangbin[1, 2, 3], LI Nan[1], LIU Chun[1, 3], SHI Beiqi[1, 4], YANG Xuan[1]

1. *Department of Surveying and Geo-Informatics*, *Tongji University*, *Shanghai* 200092 *China*;
2. *Key Laboratory of Advanced Engineering Surveying of SBSM*, *Shanghai* 2000922 *China*;
3. *Center of Spatial Information Science and Sustainable Development of Tongji University*, *Shanghai* 200092 *China*;
4. *Urban Information Research Center*, *Shanghai Normal University*, *Shanghai* 200234 *China*;

Abstract: A 3D digital image model is proposed to represent the LIDAR data. The mathematical morphology is extended to 3D and then, dilation and erosion operators are re-defined. A method combining 3D mathematical morphology with clustering analysis is developed . Sequential dilation operations and clustering analysis are introduced into the 3D point cloud to achieve the pixel-level results of point cloud. The relationships between the two parameters and data property, resolution of point cloud and the minimum distance between objects, is discussed. Two case data are used to demonstrate the feasibility of the proposed method. The result for the first dataset is compared with those from the two other methods, Mean Shift algorithm and adaptive TIN filter method. The advantages and disadvantages are summarized using segmentation evaluation factors, segmentation accuracy, and computation efficiency. Meanwhile the stabilization of proposed method is also analyzed.

Key words: LIDAR, point cloud, 3D digital Image, 3D morphology, segmentation

CLC number: TP751.1 **Document code:** A

Citation format: Wu H B, Li N, Liu C, Shi B Q and Yang X. 2011. Airborne LIDAR data segmentation based on 3D mathematical morphology. *Journal of Remote Sensing*, **15**(6): 1189–1201

1 INTRODUCTION

Light Detection and Ranging (LIDAR) is a newly developed technology system used to capture 3D spatial data in surveying and remote sensing fields. It emits controlled laser beams to obtain the reflected singles from terrain and objects in terrain. Compared with the traditional surveying methods, it is of higher accuracy, density and efficacy, and lower in cost. LIDAR have been widely used in city modeling, 3D simulation and other fields.

Point cloud is the data generated from LIDAR system. It is a dataset gathered by millions of dispersed points. Segmentation is a kind of data processing for point cloud to separate the whole data points into terrain points and non-terrain points. The current segmentation methods can be divided into two kinds, and they are by points' geometry relationship and by assisted data source.

Mathematical morphology is the first algorithm used in point cloud segmentation. This method assumes that the objects' points are higher or lower than terrain points. The point cloud is firstly converted into digital image and then the points are separated using height difference as threshold Which later been improved (Kilian, *et al*. 1996; Hug & Wehr, 1997; Zhang 2003; Zhang & Whitman, 2005). It can obtain great results in drastic rolling areas. However, for the area with uniform changes in slop, limitations still exist.

Algorithms based on slope (Vosselman, 2000; Roggero, 2001) and scan line (Sithole, 2001, 2005) are also used for segmentation. But problems will be encountered using these kinds of algorithms in applications, such as difficulty in extracting scan lines in raw data point. Thus, additional data will be required to execute such methods.

Fitting filter algorithms (Kraus & Pfeifer,1998, 2001; Elmqvist, 2001) are also important segmentation and filtering methods. These methods assume that the terrain is continuous in each sub-area. For each point in point cloud, a fitting curve will be calculated in a near threshold area and then, computes the fitting distance along the point and the fitting curve. The basis of these methods is least square.

Algorithm used in object-detection is also suggested, such as the Mean Shift algorithm (Liu & Zhang, 2009). This algorithm is based on the assumption that the mean of shift vector of certain field will move to the gradient direction of probability density. After iterations, the center of the mean of shift vector will be stable at a certain point. As it is a threshold-sensitive method, the selection

Received: 2010-07-20; **Accepted:** 2011-04-21

Foundation: Innovation Program of Shanghai Municipal Education Commission(No. 10ZZ25); Key Laboratory of Surveying and Mapping Technology on Island and Reef, State Bureau of Surveying and Mapping, China (No. 2010B12); Scientific Research Foundation of Key Laboratory for Land Environment and Disaster Monitoring of SBSM(No. LEDM2010B01)

First author biography: WU Hangbin (1983—), male, instructor, graduated from Tongji University, his research interest is processing of LIDAR data. E-mail: hb@tongji.edu.cn

of threshold will obviously affect the result. Therefore, series of thresholds as well as manual interactions are required to improve the segmentation results.

The second type of segmentation for point cloud is mainly based on the relative independent data source, such as GIS data and remote sensing imagery. It is reliable using GIS data in urban area (Lohmann, *et al*., 2000). Owing to buildings, roads, and POIs are the main objects included in GIS data, it is impossible to separate the trees and temp-objects from point cloud. Remote sensing imagery is also used to segment the raw point cloud. As the point cloud and imagery are captured separately from different platforms, it is a challenge to match the two data sources into the same coordination system (Liu & Zhang, 2005).

Considering the shortcomings of current segmentation methods, a new algorithm which hires the 3D mathematical morphology and clustering analysis is proposed in this paper. Point cloud will be firstly converted into the 3D digital imagery. After that, 3D mathematical morphology is introduced into the 3D digital imagery. Then, clustering analysis is used to process the morphological data to obtain the segmentation results.

2 3D DIGITAL IMAGERY OF POINT CLOUD AND 3D MATHEMATICAL MORPHOLOGY

2.1 3D digital imagery of point cloud

Traditional grey imagery can be regarded as a 2D function $f(x, y)$, where x, y is the coordination and the f value in location (x, y) can be regarded as the luminance. Color image is a combination of grey images.

The coordination (x, y) and its function value (f) are continuous. In order to make it possible for computer to store and process the images, discretization is necessary to convert the imagery from continuation to digital forms. In digital image processing, we call discretization for coordinate as sampling and discretization for function value as quantization. When x and y are limited and discrete, the imagery can be regarded as 2D digital imagery or grey digital image. Thus, a 2D imagery will be expressed as:

$$f=\begin{bmatrix} f(0,0) & f(0,1) & \cdots & f(0,N-1) \\ f(1,0) & f(1,1) & \cdots & f(1,N-1) \\ \cdots & \cdots & \cdots & \cdots \\ f(M-1,0) & f(M-1,1) & \cdots & f(M-1,N-1) \end{bmatrix} \quad (1)$$

where M is the row number of the image, N is column number of the image.

2D image can only express and handle 2D data composed by plane coordinate information and its attributes. For remote sensing processing, more data need to be processed, such as hyper-spectral data, intensity, *etc*. Therefore, 3D digital imagery is proposed to extend the usage of imagery.

Point cloud is mainly consisted of spatial data (x, y, z) and intensity. 3D imagery of point cloud is sampled by a three-dimensional coordinate system, and thus a three-dimensional matrix will be established by discretizing the attribute of laser spot in the pixels. To facilitate the application, the axis of the 3D digital image of point cloud is defined as (Fig.1): coordinate origin is at the bottom left of the data set, the positive direction of row i is along the east, the positive direction of column j is along the north, the k direction is the positive direction of elevation. It is a right-handed coordinate system. Therefore, 3D digital imagery of point cloud can be represented by $f(i, j, k)$.

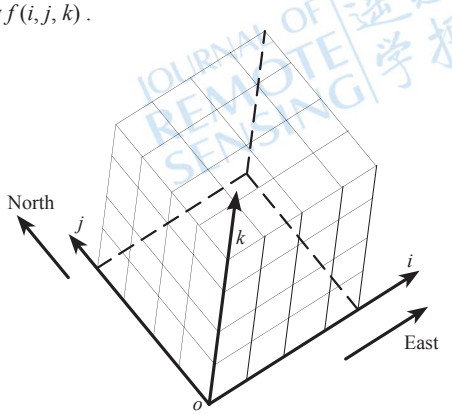

Fig. 1 Coordinate system definition of a 3D digital image based on point cloud

Each pixel of the 3D digital imagery represents a cubic in the space. The attributes of the pixel are expressed by the amplitude of the pixel. The weighted method or middle point method of laser point within the pixel can be used to obtain the attribute of the pixel.

2.2 3D mathematical morphology

The fundamental of mathematical morphology is collecting imagery information by structural elements. The relationship and structural character of each part of imagery can be learnt from keeping the structural elements moving in the imagery (He, *et al*., 2006). 3D mathematical morphology operations are similar to the 2D mathematical morphology operations. It gets structural character through the moving of 3D structural elements in the imagery. Erosion and dilation are two basic operations in morphology. As it is similar with the definition of 2D erosion and dilation, the 3D morphology is defined as:

Assumed that B is a 3D structural element, X is a 3D digital imagery, B_a will be obtained after B moves a.

If B_a is included in X, then point a is noted. The point consisted of a, is called the result that X is eroded by B. And it can be represented as the formula: $E(X)=\{a|B_a \subset X\}$, Θ stands for erosion operation, it is expressed as $E(X)=X\Theta B$.

Dilation operation can be regard as dual operation of erosion. B_a is obtained after B moves a, If B_a is included in X, then point a is noted. The point set consisted of a, is called the result that X is dilated by B. The formula is expressed as $D(X)=\{a|B_a \uparrow X\}$. $\oplus$ is used to represent dilation, it can be expressed as: $D(X)=X \oplus B$.

Convolution is a method used in the processing of imagery which is similar with matrix calculations. The processing of imagery in pixel level can be considered as combination of convolutions. Convolution can be regarded as a sum of imagery multiplies convolution kernel (convolution operator or convolution matrix) by its weights at the corresponding position. The pixel value of original image will be replaced by the result of convolution. This method is widely used in the imagery processing.

3D erosion and dilation operation can also be represented by convolution of 3D matrix. 3D binary imagery, for instance, its con-

volution can be represented as: dilation is calculated by convolution $\boldsymbol{R}$ and initial imagery, if the result is larger than 0, set the pixel value as 1, if not, set 0; and for erosion operation, if the result of convolution is less than 27, set 0, if not, set 1.

$$\boldsymbol{R}=(\boldsymbol{R}_{i,j,k}=1),(i=1–3,\ j=1–3,\ k=1–3) \tag{2}$$

3 SEGMENTATION MODEL AND PARAMETERS

3.1 Segmentation model

The whole points in point cloud can be mainly divided as terrain points and non-terrain points. Terrain points are the points located in bare earth, such as hill points, road points, soil points. Non-terrain points are the points that are locates in objects which are higher or lower than terrain points, such as noisy points, building points, tree points, wall points *etc*. The method proposed in this paper uses 3D digital image model and 3D mathematical morphology to make sure that the points belong to the same object will be connected in 3D image after processing. And then clustering analysis is hired to obtain the segmentation results.

The flowchart of the proposed method is described as Fig. 2. Let G be the sampled 3D digital image. A new image, G1, will be obtained after dilating G. As the point distance between points that located in the same object is shorter than that between different objects, therefore, during dilation processing, the pixels belonged to the same object will be connected firstly, and meanwhile the pixels belonged to different object will keep separating. Then, clustering analysis is hired to obtain connected points as the segmentation results.

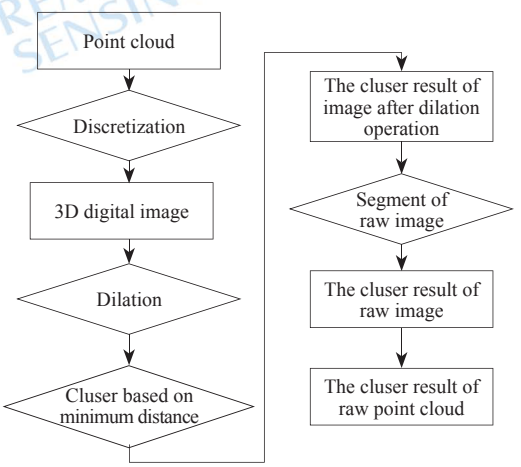

Fig. 2 The flowchart of proposed method

3.2 Segmentation parameters

Cellsize for sampling and iteration times (n) are the two parameters of proposed method. The resolution of the 3D digital image is determined by cellsize, while the times for dilation are determined by n.

Let d_1 be the resolution of point cloud along flight direction, d_2 be the resolution along scan line, d_3 be the minimum height difference between terrain points and objects' points, and d_4 be the minimum height difference between adjacent objects. The two parameters, cellsize and n, could be evaluated by these four values.

During each dilation operation, any pixel of the 3D image will be expanded along six neighborhoods. Thus the maximum width of a pixel is $(2n+1)\times cellsize$ after n times of dilation. To separate different kind of object points, the same object points should be stretched. Thus inequality Eq. (3) should be satisfied:

$$(2n+1)\times cellsize \geqslant \max(d_1,d_2) \tag{3}$$

Meanwhile, different kinds of object points, terrain and object points, will remain separated, then inequality Eq. (4) should be satisfied:

$$(2n+2)\times cellsize \leqslant \min(d_3,d_4) \tag{4}$$

So, the relationship of cellsize and iteration times can be represented as inequality Eq. (5):

$$\frac{\max(d_1,d_2)}{(2n+1)} \leqslant cellsize \leqslant \frac{\min(d_3,d_4)}{(2n+2)} \tag{5}$$

In the inequality Eq. (5), n is integer. In fact, the value of n can be 1, 2, 3, *etc*., and the range of cellsize parameter can be obtained.

4 EXAMPLES ANALYSIS

4.1 Experimental data

The experimental data are two sets of point cloud which cover different kinds of surface. The first data is downloaded from the website (http://isprs.ign.fr/packages/packages_en.htm) of the 8th work group of III committee of ISPRS. The data was captured at 2003, including 108092 points. It mainly includes buildings, ground points, vegetation, fence, vehicles, *etc*.. This kind of data represents typical urban areas (Fig. 3).

Fig. 3 Imagery of first dataset

The second data is downloaded from the website (http://metadataexplorer.gis.state.oh.us/metadataexplorer/explorer.jsp) of Digital projects of Ohio in USA, collected by ALS50 system in 2006. It includes 47787 points and locates in the mountains of north Ohio. The main objects within this area are mainly mountains, trees, detritus, factory building, pendants, ditches *etc*.. The data are shown as Fig. 4:

Fig. 4 Imagery of second dataset

4.2 Segmentation result

For the first data, the resolution along flight line is about 1.8 m, the maximum resolution along scan line direction is about 0.09 m, the minimum distance between buildings is 2.3 m, the minimum height difference between terrain points and object points is 3.3 m.

According to Eq. (5), use n=1, *cellsize*=0.55 and n=2, *cellsize*=0.35 to process the point cloud, and results are shown as Fig. 5 and Fig. 6, respectively. The numbers in Fig. 5 and Fig. 6 stand for the segmentation object serial numbers which are sorted by point count.

Fig. 5 Result by first set of parameters for first dataset

Fig. 6 Result by second set of parameters for first dataset

According to Eq. (5), use n=1, *cellsize*=0.55 as experiment parameter to segment the second data, and the result is shown as Fig. 7.

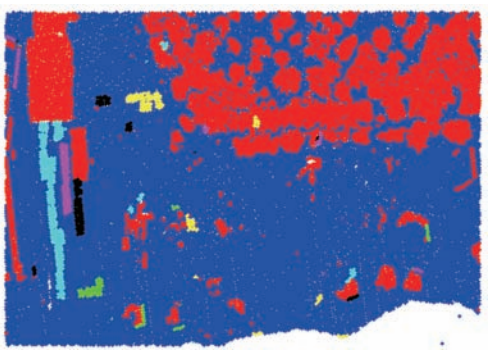

Fig.7 Segmentation result for second dataset

By comparing Fig. 3 and Fig. 5, Fig. 4 and Fig. 7, it is obvious that the method we proposed is very effective to detect dense point cloud areas both in urban and mountainous areas.

4.3 Comparison analysis

4.3.1 Experiment for comparison

Comparison analysis is conducted using the first dataset.

As no prior knowledge of experiment area is available, Mean Shift algorithm, adaptive TIN filter method is used to segment the point cloud and conduct a comparison with proposed method. Firstly, raw points are processed by the Mean Shift algorithm.

The major parameter of the Mean Shift algorithm is bandwidth. Select a random point as starting point, search points within the bounds of bandwidth, and calculate the vectors and mean vector between searched points and starting point. Then move the search center from original starting point to the mean center. Then use bandwidth to research points, calculate the mean center and move the search center to new mean center again. Stop the iteration until the center is steady.

After several experiments, we found that it reaches good results when bandwidth is between 0.15 and 0.20. The results by these parameters are shown as Fig. 8 and Fig. 9.

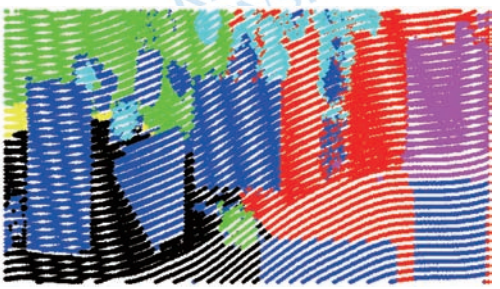

Fig. 8 Result using the Mean Shift when *bandwidth*=0.20

Fig. 9 Result using the Mean Shift when *bandwidth*=0.15

TIN filter method is also hired to process the data, the two main parameters, maximum building size and maximum angle hypsography are settled as 55 m and 88°, respectively. The segment result is shown in Fig. 10.

From Fig. 8 and Fig. 9, the Mean Shift algorithm can detect geographical objects in the point cloud. However, it is obviously that it does not perform well as the proposed method in term of the integrity of segmentation and result of separating the bulky objects. The segmentation result could be better if the manual adjustment is added.

According to Fig. 10, adaptive TIN filter method is effective to extract bulky buildings, but small buildings are often regarded as High Vegetation. Moreover, it is highly sensitive to the terrain. The small waves of terrain will usually be identified as Low Vegetation. Since the adaptive TIN filter method is conducted on all data, the parameter is applied on the whole area without considering local situation. Therefore, in practice, the classification can be improved by adjusting parameters.

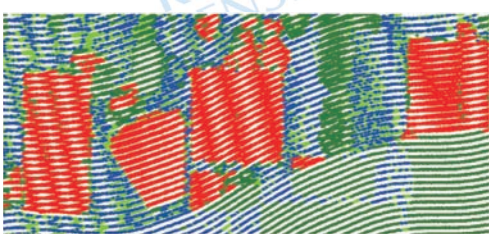

Fig. 10 Result by adaptive TIN filter algorithm

4.3.2 *Quality evaluation*

The quality of three methods is evaluated by four indexes, uniformity (*UN*), region contrast (*GC*), fuzzy entropy (*E*), shape measurement (*SM*), all which are widely used in imagery segmentation. Moreover, function F is used to evaluate segmentation quality comprehensively, where

$$F=UN\times GC\times E\times SM \tag{6}$$

When the value of *UN*, *GC*, *E*, *SM* and F is higher, it denotes the better segmentation result. The parameters of method in this paper, including the Mean Shift algorithm and the adaptive TIN filter method, are listed in Table1.

According to Table1, the similar *UN* values indicate that the segmentation of three methods all conform to uniformity. *GC* of the proposed method slightly lower than that of the Mean Shift algorithm and the adaptive TIN filter method, that means, the *GC* of proposed method is not as good as the other two methods. However, in terms of *E* and *SM*, the proposed method is much better than that of the Mean Shift algorithm and the adaptive TIN filter method. As the comprehensive analysis of evaluation parameters, the segmentation result of proposed method is better than the results conducted by both the Mean Shift algorithm and the adaptive TIN filter method

Table 1 Evaluation table of segmentation result

Methods	parameters	*UN*	*GC*	*E*	*SM*	*F*
Proposed method	*n*=1	0.978	0.188	0.733	4.158	0.552
	n=2	0.979	0.191	0.725	3.503	0.476
Mean Shift algorithm	*bandwidth*=0.20	0.975	0.308	0.464	0.148	0.021
	bandwidth=0.15	0.979	0.289	0.449	0.192	0.024
Adaptive TIN filter method	—	0.979	0.306	0.505	0.002	0.0004

Table 2 Statistics of segmentation accuracy for first dataset

Methods	Parameters	Terrain points	
		Commission rate/%	Omission rate/%
Proposed method	*n*=1	0.95	1.39
	n=2	0.83	2.10
Mean Shift algorithm	*bandwidth*=0.20	0.00	8.69
	bandwidth=0.15	0.16	6.11
Adaptive TIN filter method	—	17.37	19.65

4.3.3 *Accuracy Analysis*

The manual segmentation of first dataset is added assisted by imagery. Then we evaluate the segmentation accuracy of terrain points using the proposed method, the Mean Shift algorithm and the adaptive TIN filter method. The results are shown in Table 2.

As shown in Table 2, in terms of the accuracy of segmentation, the proposed method and the Mean Shift algorithm can both achieve satisfactory effects with all commission rates within 1%. And in term of integrity of segmentation, the omission rate of proposed method is obviously lower than the Mean Shift algorithm and the adaptive TIN filter method, which indicates that the integrity of segmentation of proposed method is better than the other two methods.

From Table 3, we can conclude that the commission and omission error is low, which ensures the proposed method to be used as general method in point cloud segmentation.

Table 3 Segmentation accuracy for second dataset

Methods	Parameters	Terrain points	
		Commission rate/%	Omission rate/%
Proposed method	*n*=1	0.11	1.42

4.3.4 *Analysis of Operation Efficiency*

The efficiency of three methods is analyzed by recording the time consuming when running algorithms for the first dataset. Proposed method and Mean Shift algorithm are operated in Matlab2008A, and CPU of computer is Intel P4 2.8 GHZ, the memory is 4 G, and adaptive TIN filter method is operated in MicroStation. The running times of each method are recorded as shown in Table 4.

As is known from Table 4, the proposed method is obviously of higher efficiency than the Mean Shift algorithm, while barely higher than adaptive TIN filter method.

Table 4 Staticastic of time consuming for each method

Methods	Parameters	Running time/s
Proposed method	*n*=1	4.7
	n=2	5.5
Mean Shift algorithm	*bandwidth*=0.20	26.8
	bandwidth=0.15	53.2
Adaptive TIN filter method	—	5.5

4.4 Stabilization analysis

Stabilization is analyzed according to the comparison of two results of proposed method using different parameters. As shown in Fig. 5 and Fig. 6, the results two segmentations are consistent. The statistics of point count of major area of two segmentation results are listed in Table 5. The change rate referrs to the change between segmentation points of two results of the same area.

According to the Fig. 5, Fig. 6 and Table 5, the 8th region of segmentation result using *n*=1, *cellsize*=0.55 is divided into region 8 and region 12 when *n*=2, and *cellsize*=0.35.

It also can be seen from Table 5, except the 6th region (3.3%), the change rate of other regions is around 1%, which shows good stabilization of the proposed method, and the results remain simi-

lar by using different parameters. Meanwhile, it indicates that the model of calculating values of the parameter is effective.

Table 5 Staticastic of segmentation result using the proposed method

Parameters	n=1	Parameters	n=2	Change rate/%
Number	Point count	Number	Point count	
1	45514	1	44910	1.3
2	13690	2	13622	0.5
3	12335	3	12214	0.1
4	12137	4	12063	0.6
5	5937	5	5937	0.0
6	3302	6	3193	3.3
7	2609	7	2608	0.0
8	3193	8	2342	1.4
		12	807	
9	2141	9	2141	0.0
10	1580	10	1563	1.1
11	1211	11	1211	0.0

5 CONCLUSION

Considering the shortcomings of current LIDAR segmentation method, a new segmentation method based on 3D mathematical morphology is presented in this paper. It is combined with dilation of 3D digital imagery of point cloud and cluster analysis. The sampling interval and times dilation can be obtained from point cloud and trajectory design data, which are the keys for the proposed method. Compared with the Mean Shift algorithm and the adaptive TIN filter method, the result of proposed method is better in terms of integrity, accuracy, running efficiency and stabilization, and therefore, the proposed method can be generally used to point cloud segmentation.

The main shortcoming of the proposed method is that the adjacent objects with similar height, such as buildings and its neighbored trees, cannot be properly separated. In fact, it is a common shortcoming of the method based on point cloud data. The segmentation result could be better if this kind of data are supported by other information, such as an image.

REFERENCES

Elmqvist M. 2001. Ground estimation of laser radar data using active shape models. *Proceedings*, *OEEPE Workshop on Airborne Laser Scanning and Interferometric SAR for Detailed Digital Elevation Models*, Stockholm, Sweden, Vol. XXXX

Haala N, Brenner C and Stätter C. 1998. An integrated system for urban model generation. *International Archives of Photogrammetry and Remote Sensing*, (2): 77–84

He X H, Zhou Y Y, Wang J Y, Zhou H. 2006 Image Processing Using Matlab 7.x. Beijing: The People's Posts and Telecommunications Press

Hou G X, Bi D Y and Wu C K. 2000. Researches on evaluation methods for image segmentation. *Journal of Image and Graphics*, **5**(1): 39–43

Hug C and Wehr A. 1997. Detecting and identifying topographic objects in imaging laser altimetry data. *International Archives of Photogrammetry and Remote Sensing*, **32**(3-4W2): 19–26

Kilian J, Haala N and Englich M. 1996. Capturing and evaluation of airborne laser scanner data. *International Archives of Photogrammetry and Remote Sensing, Vienna*, **32**(B3): 383–388

Kraus K and Pfeifer N. 1998. Determination of terrain models in wooded areas with ALS data. *ISPRS Journal of Photogrammetry and Remote Sensing*, **53**(4): 193–203 DOI: 10.1016/S0924-2716-(98)00009-4

Kraus K and Pfeifer N. 2001. Advanced DTM generation from LIDAR data. *International Archives of Photogrammetry and Remote Sensing*, **XXXIV**(3/W4): 23–30

Li H, Li D R, Huang X F and Zhong C. 2009. Advanced adaptive TIN filter for LIDAR point clouds data. *Science of Surveying and Mapping*, **34**(3): 39–40

Liu C and Zhang Y L. 2009. Extraction of 3d feature from lidar data fused with aerial images using improved mean-shift algorithm. *International conference on Geo-spatial Solutions for Emergency Management and the 50th Anniversity of the Chinese Academy of Surveying and Mapping*, *Beijing*, *China,* **33**(Part 7-C4): 20–24

Liu J N and Zhang X H. 2005. Classification of laser scanning altimetry data using laser intensity. *Geomatics and Information Science of Wuhan University*, **30**(3): 189–193

Lohmann P, Koch A and Schaeffer M. 2000. Approaches to the filtering of laser scanner data. *International Archives of Photogrammetry and Remote Sensing*, **33**(B3): 540–547

Roggero M. 2001. Airborne laser scanning: clustering in raw data. *International Archives of the Photogrammetry and Remote Sensing*, **34**(B3-W4): 227–232

Sithole G. 2001. Filtering of laser altimetry data using a slope adaptive filter. *International Archives of Photogrammetry and Remote Sensing*, **34**(3-W4): 203–210

Sithole G. 2005. Segmentation and Classification of Airborne Laser Scanner Data. Delft: Technical University of Delft

Vosselman G. 2000. Slope based filtering of laser altimetry data. *International Archives of Photogrammetry and Remote Sensing*, **33**(B3): 935–942

Weidner U and Forstner W. 1995. Towards automatic building extraction from high resolution digital elevation models, *ISPRS Journal of Photogrammetry and Remote Sensing*, **50**(4): 38–49

Xu J H. 2002. The Mathematical Methods in Contemporary Geography. 2nd ed. Beijing: Higher Education Press

Zhang K Q, Chen S C, Whitman D, Shyu M L, Yan J H and Zhang C C. 2003. A progressive morphological filter for removing nonground measurements from airborne LIDAR data. *IEEE Transactions on Geoscience and Remote Sensing*, **41**(4): 872–882

Zhang K Q and Whitman D. 2005. Comparison of three algorithms for filtering airborne LIDAR data. *Photogrammetric Engineering and Remote Sensing*, **71**(3): 313–324

机载激光扫描数据分割的三维数学形态学模型

吴杭彬[1,2,3]，李楠[1]，刘春[1,3]，施蓓琦[1,4]，杨璇[1]

1. 同济大学测量与国土信息工程系，上海 200092；
2. 现代工程测量国家测绘局重点实验室，上海 200092；
3. 同济大学空间信息科学及可持续发展应用中心，上海 200092；
4. 上海师范大学城市信息研究中心，上海 200234

摘　要：机载激光扫描点云的三维数字图像表达模型将二维形态学运算推广至三维，给出基于三维数字图像的膨胀和腐蚀运算方法。针对点云三维数字图像，提出基于三维数学形态学和聚类分析的分割方法。将点云三维数字图像进行膨胀和聚类分析，依据聚类结果得到点云的分割结果。讨论了本方法两个参数与点云分辨率、地物间隔之间的关系。选用两套实例数据进行实验，并将第一套数据计算结果与Mean Shift算法、渐进三角网加密算法进行比较，从分割评价因子、精度、计算效率等方面分析本文方法与其他两种方法的优劣，最后分析了本文方法的稳定性。

关键词：机载激光扫描，点云，三维数字图像，三维形态学，分割

中图分类号：TP751.1　　**文献标志码：**A

引用格式：吴杭彬，李楠，刘春，施蓓琦，杨璇. 2011. 机载激光扫描数据分割的三维数学形态学模型，遥感学报，**15**(6): 1189–1201
Wu H B, Li N, Liu C, Shi B Q and Yang X. 2011. Airborne LIDAR data segmentation based on 3D mathematical morphology. *Journal of Remote Sensing*, **15**(6): 1189–1201

1　引　言

激光扫描获取地面三维数据的LIDAR(Light Detection And Ranging)系统是测绘、遥感领域的高新技术系统之一。该系统发射受控制的激光以照射地面和地面上的目标，可全天时获取地面三维数据。相比传统测量方法，具有高精度、高密集、高效率、低成本和大数据量的优点，在城市建模、三维仿真等领域应用广泛。

从LIDAR系统获取的原始数据经处理后得到点云。点云是离散的数据点集合，可达到数十万至上千万点。点云数据处理和应用的基础是点云分割。点云分割是指将点云数据按所属的性质分为地面点或具体的地形点。点云分割按方法可分为两种：依据点云自身几何关系的分割和依据其他数据的分割。

依据点云自身几何关系的方法中，二维形态学的方法(Weidner和Forstner，1995)最先用于点云分割。该方法假设目标点高于或者低于一般的地面点云，将点云转换为数字图像后根据高程差异分割不同区域的点云。Kilian等人(1996)、Hug和Wehr(1997)、Zhang等人(2003)以及Zhang和Whitman(2005)改进了形态学方法。形态学方法意义直观、便于操作和实现，在一些地形起伏较大的区域，分割效果明显。然而在坡度均匀变化的区域，形态学计算的方法也存在一定的限制，分割结果还有待改善。

坡度方法(Vosselman，2000；Roggero，2001)和点云扫描线方法(Sithole，2001，2005)也用于点云分割。这些方法都能部分解决点云的分割问题，然而在实际应用过程中，也存在一些限制。如无法获取扫描线信息等。

拟合滤波(Kraus和Pfeifer，1998，2001；Elmqvist，2001)也是重要的点云数据分割和滤波方法。这种方

收稿日期：2010-07-20；**修订日期：**2011-04-21

基金项目：上海市教育委员会科研创新项目(编号: 10ZZ25)；海岛(礁)测绘技术国家测绘局重点实验室(编号: 2010B12)；国土环境与灾害监测国家测绘局重点实验室(编号: LEDM2010B01)

第一作者简介：吴杭彬 (1983—)，男，讲师，2010年毕业于同济大学测量系，获大地测量学与测量工程博士学位。现从事机载激光扫描数据处理领域研究。E-mail: hb@tongji.edu.cn。

法假设地面是分段连续的，对点云中的每个点的局部邻域计算回归平面，并计算点到回归平面距离的方法实现点云分割。这一方法的数学基础是平面拟合的最小二乘平差。

目标检测领域的一些聚类算法也被引入点云数据分割过程，如Mean Shift算法等(Liu和Zhang，2009)。这一算法依据某一邻域的偏移向量的平均值指向概率密度梯度方向并最终收敛至某一特定点的原理，将收敛于同一点的激光点作为同一对象分割点云数据。由于Mean Shift算法是阈值敏感的方法，因此阈值的选择对计算结果影响明显。此外大型物体(如大型建筑、地面点等)用Mean Shift算法分割时往往会分成多区域。因此，该方法分割数据时，一般需多次调整并辅以较多的人工判别才能得到较好的分割结果。

点云分割的第2类方法是利用其他数据，如GIS数据、影像等。GIS数据用于点云分割在城市等数据充分区域较为可靠(Lohmann 等，2000)，然而由于GIS数据一般只具备建筑、道路等数据，因此只能得到建筑、道路的分割结果，而无法分割树木、临时堆积物等地物。融合多光谱数据和激光扫描数据进行数据分割和分割也有人进行过研究(Haala 等，1998)，但该方法由于两种数据是分别独立获取的，在进行匹配时有一定难度，也难以确定其边界(刘经南和张小红，2005)。

针对目前点云数据分割方法的缺点，本文提出基于三维数学形态学和聚类分析的分割方法。将点云数据首先以一定采样间隔转换成三维数字图像，然后对三维数字图像进行形态学运算，最后对形态学运算结果进行聚类分析，得到点云分割结果。

2 点云三维数字图像和三维数学形态学

2.1 点云三维数字图像

传统意义上的图像可定义为一个二维函数$f(x,y)$。其中，x,y是空间平面坐标，f在任何坐标点(x,y)处的振幅称之为图像在该点的亮度。灰度是用来表示黑白图像亮度的术语，彩色图像是由单个二维图像组合而成。

图像关于 x,y 坐标以及振幅都是连续的，要将连续图像转换成数字形式，就要求离散化坐标数据和振幅。将坐标数据值离散化的过程称之为采样，将振幅离散化的过程称之为量化。当 x,y 以及振幅都是有限且离散的量时，称该图像为二维数字图像 $f(i,j)$。因此，二维数字图像可以用式(1)表示：

$$f=\begin{bmatrix} f(0,0) & f(0,1) & \cdots & f(0,N-1) \\ f(1,0) & f(1,1) & \cdots & f(1,N-1) \\ \cdots & \cdots & \cdots & \cdots \\ f(M-1,0) & f(M-1,1) & \cdots & f(M-1,N-1) \end{bmatrix} \tag{1}$$

式中，M和N分别代表图像的行和列。

在遥感数字图像处理中，二维数字图像只能表达由平面坐标和属性信息组成的数据，无法同时表达点云的高程信息和属性信息。在表达由三维空间坐标及相关的属性组成的点云数据时，二维数字图像存在一定的限制和约束。针对二维数字图像的这一缺点，本文提出点云的三维的数字图像表达方法。

点云数据一般由地面点的空间坐标(x,y,z)以及回光强度值信息(*intensity*)组成。点云三维数字图像是将点云按三维坐标进行采样，并根据像元内激光点的某一属性进行量化得到的三维矩阵。为使用方便，如图1所示，约定点云三维数字图像的坐标轴：坐标原点位于数据集的左下方，往东方向为行序号i的正方向，北方向为列序号j的正方向，高程的正方向作为k方向，组成右手坐标系。因此，三维数字图像可用$f(i,j,k)$表示。

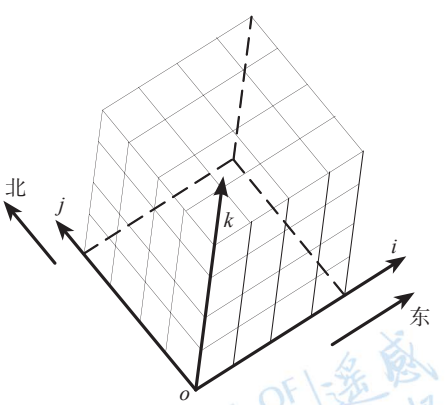

图1 点云三维数字图像的坐标系约定

三维数字图像的每个像元对应了空间中的一个立方体，像元的振幅表示该像元的属性信息。像元的属性值可以对像元内部激光脚点采用加权法、中间点法等方法确定。

2.2 三维数学形态学

数学形态学的基本原理是利用结构元素收集图像

的信息，当结构元素在图像中不断移动时，可以考察图像各部分之间的相互关系，并了解各部分的结构特征(贺兴华 等，2006)。三维数学形态学运算与二维形态学运算类似，通过三维的结构元素在图像中移动从而获取结构特征。腐蚀和膨胀是形态学的两种基本运算。与二维腐蚀和膨胀运算的定义类似，给出三维形态学运算的定义：

假设B为三维结构元素，X为三维的数字图像，将B平移a后，得到B_a。若B_a包含于X，则记下a点，所有满足上述条件的a点的集合，称为X被B腐蚀的结果，表示为$E(X)=\{a|B_a\subset X\}$。用Θ表示腐蚀运算，则记为$E(X)=X\Theta B$。

膨胀运算可以看作是腐蚀运算的对偶运算。将结构元素B平移a后，得到B_a，若B_a击中X，则记下a点，所有满足上述条件的a点集合称之为X被B膨胀的结果。表示为$D(X)=\{a|B_a\uparrow X\}$。用$\oplus$表示膨胀运算，则记为$D(X)=X\oplus B$。

卷积运算是图像处理中的一种计算方法，与矩阵的运算有一定的相似性。像元级别的图像处理分析可认为是卷积运算的组合。卷积运算可看作是图像与卷积核(也称卷积算子，卷积矩阵)在对应位置加权求和的过程，将图像局部区域的每个像元与卷积核的每个元素对应相乘之和作为区域中心像元的新值。这种方法在图像处理方面应用广泛。

三维的腐蚀和膨胀运算也可以用三维矩阵的卷积运算表示。以三维的二值图像为例，采用卷积方法可以表示为：膨胀是用卷积矩阵R和原图像进行卷积计算，如果结果大于0就将该像元置为1，否则赋0；而腐蚀过程则是将卷积结果小于27的像元置为0，否则赋1。其中，

$$\boldsymbol{R}=(\boldsymbol{R}_{i,j,k}=1),(i=1\text{–}3,j=1\text{–}3,k=1\text{–}3) \tag{2}$$

3 分割模型和参数

3.1 分割模型

点云主要包括地面点和地形点。地面点即为裸露地表点，包括山体、道路、裸露土壤等；地形点包括与地面存在一定高差的点，如噪声点、建筑、树木、围墙、电力线等。本文分割方法原理是利用点云三维数字图像和三维形态学运算，使同一对象的激光点在点云三维图像的像素级别相连，然后通过聚类分析获得相连像素即可得到点云分割结果。

点云离散化采样后的三维数字图像经膨胀得到的新的数字图像中，由于相同的地物对象的不同像元距离小，因此在膨胀过程后，已经在像元级别上相连。而不同地物对象的像元点距离大，膨胀运算将缩小像元之间的距离，但仍然难以在像元级别上相连。形态学膨胀后，采用聚类分析方法对不同地物对象。常见的聚类分析方法有系统聚类法、动态聚类法和模糊聚类法等(徐建华，2002)，具体的计算原则有最小距离、直接聚类、最大距离样本、K均值聚类、迭代自组织(ISODATA)等。本文采用最小距离法对膨胀后的数字图像进行聚类。最后在聚类的结果上，指导原有三维数字图像和点云数据的分割。流程如图2所示。

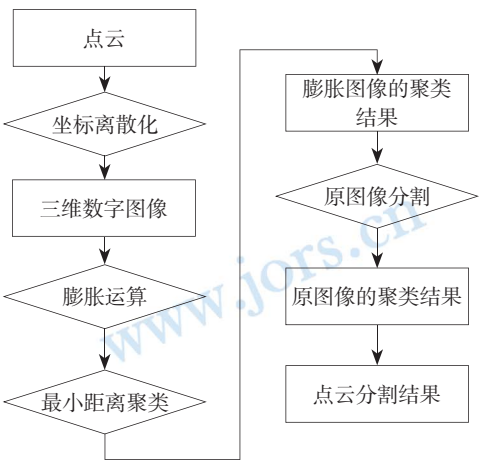

图2 本文方法的流程图

3.2 分割参数选取

点云数据离散化采样间隔*cellsize*和形态学运算次数n是本方法的主要参数。采样间隔给定了依据点云得到数字图像的三维分辨率；形态学运算次数则主要用于指定对三维图像进行膨胀运算的次数。

设点云数据的航向分辨率为d_1，扫描线方向的最大分辨率为d_2；点云中，地面点与地物点之间的最小高差为d_3，相连地物之间的最小距离为d_4。分割模型的两个参数与这4个点云的参数存在一定的关系。

在三维形态学膨胀运算过程后，三维图像的每个像元会在其六邻域各扩展一个像元。因此任一像元经n次膨胀后，最大宽度为$(2n+1)\times cellsize$。为达到分割不同地物激光点的效果，相同地物的激光点应连接成片，则需满足式(3)：

$$(2n+1)\times cellsize\geqslant\max(d_1,d_2) \tag{3}$$

同时，不同地物的激光点、地面点与地物点仍处于分

离状态，则需满足式(4)：

$$(2n+2)\times cellsize \leqslant \min(d_3,d_4) \tag{4}$$

整理后，得到采样间隔与膨胀次数的关系如式(5)：

$$\frac{\max(d_1,d_2)}{(2n+1)} \leqslant cellsize \leqslant \frac{\min(d_3,d_4)}{(2n+2)} \tag{5}$$

式中，n为整数，实际计算过程中可以以1、2、3等值代入，*cellsize*参数即可指定其选取范围。

4 实例分析

4.1 实验数据

选取两套数据具备不同地物覆盖条件的点云数据进行分析。第1套数据下载自ISPRS第3委员会第8工作组网站(http://isprs.ign.fr/packages/packages_en.htm)，采集时间约为2003年，共108092个点，主要存储了房屋、地面点、植物、围墙、车辆等地物，该类型的数据在城市区域较为典型具有一定代表意义。数据区域如图3所示。

图3 第1套数据的影像图

第2套数据下载自美国俄亥俄州Digital Ohio项目网站(http://metadataexplorer.gis.state.oh.us/metadataexplorer/explorer.jsp)，由ALS50系统于2006年采集，共47787个点，位于俄亥俄州北部山区，主要存储了山体、树木、堆积物、厂房、吊塔设备、沟渠等地物的数据。数据区域如图4所示：

图4 第2套数据的影像图

4.2 分割结果

对第1套数据进行分析，点云的航向分辨率约为1.8 m，扫描线方向的最高分辨率约为0.09 m；地物间(建筑物)的最小距离为2.3 m，地物点与地面点之间的最小高差为3.3 m。根据式(5)，分别选取n=1，*cellsize*=0.55以及n=2，*cellsize*=0.35两套参数对点云进行处理，得到点云分割结果如图5和图6所示。图5和图6中的数字表示按照区域点数排序后的分割对象序号。

图5 第1套数据采用第1套参数的分割结果

图6 第1套数据采用第2套参数的分割结果

根据式(5)，采用n=1，*cellsize*=0.55作为实验参数，对第2套数据进行分割，得到分割结果如图7。

比较图3与图5、图6，图4与图7可看出，无论在不同的地物覆盖条件的城市或山区，本文方法都能较好地检测数据集中的树木、建筑物、堆积物和机械设备等地物。

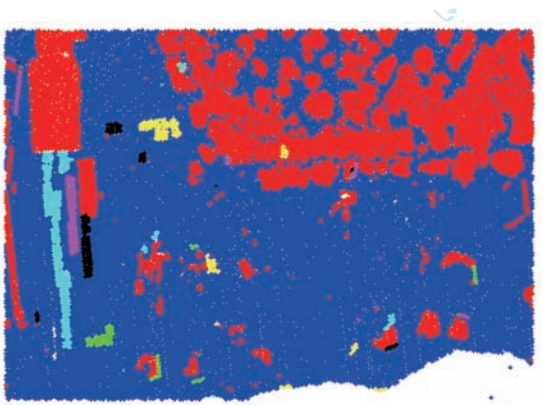

图7 第2套数据处理结果

4.3 对比分析

4.3.1 比较实验

取第1套数据进行对比分析实验。

因无实验区域的先验知识，对原始实验数据分别采用Mean Shift算法(Liu和Zhang，2009)和渐进加密三角网算法(李卉 等，2009)进行分割。首先对原始数据采用Mean Shift算法进行处理。

Mean Shift算法的主要参数为核宽窗。核宽窗指算法进行时的搜索窗口大小。分割时，首先随机指定一个点作为迭代起始点，然后在核宽窗范围内查找点云，计算这些点云与起始点的向量和向量均值，将起始点按向量均值偏移后，重新按照核宽窗范围查找点云，如此多次迭代后达到稳定，分割的点作为同一类别。

多次处理后，总结核宽窗参数在0.15和0.20之间的分割效果最好。核宽窗选用0.20和0.15的处理结果分别如图8、图9所示。

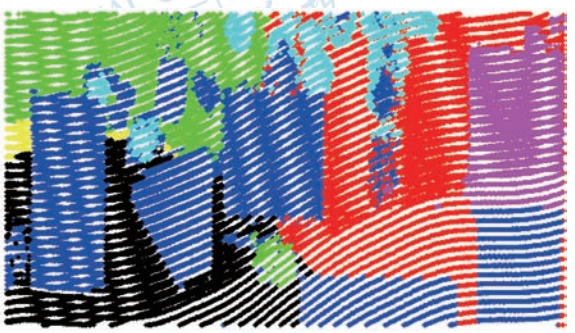

图8 核宽窗为0.20的Mean Shift分割结果

图9 核宽窗为0.15的Mean Shift分割结果

采用渐进加密三角网算法对原始数据进行处理，设置最大建筑物周长为55 m，地形起伏最大角度为88° ，得到分割结果如图10所示：

从图8、图9可看出，采用Mean Shift算法也可以有效识别点云中的地物对象，然而分割结果的整体性和大型地物分割结果方面明显不如本文方法，Mean Shift方法须辅以较多的人工判读和处理，才能得到好的分割结果。

从图10可看出，基于渐进三角网加密算法在大型建筑物提取方面有较好的效果，然而小型建筑物往往会被误分类为高层植物类(High Vegetation)。此外，渐进加密三角网算法对地形具有高度敏感性，地形上的小起伏也往往被误识别成低层植被类(Low Vegetation)。可以看出，渐进三角网加密算法是针对全局数据的算法，参数一旦指定，就会以参数应用于所有区域，而不考虑局部区域的实际情况。因此实际应用中，往往需要依据前次结果，多次调整参数，才能得到较好的分类结果。

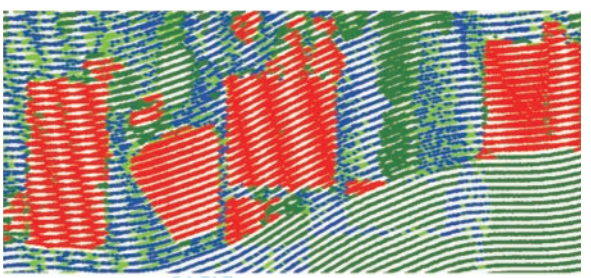

图10 渐进三角网加密算法处理结果

4.3.2 质量评价

对3种方法处理结果直接采用影像分割方法中广泛采用的区域一致性(*UN*)、区域对比度(*GC*)、模糊熵(*E*)、区域形状测度(*SM*)等4个方面对分割结果进行质量评价，并采用综合评定函数(*F*)综合评价(侯格贤 等，2000)分割质量。其中，

$$F=UN\times GC\times E\times SM \tag{6}$$

式中，*UN*、*GC*、*E*、*SM*以及*F*值越大，表明分割结果越好。表2给出了本文方法的各个指标参数以及基于Mean Shift分割方法和渐进三角网加密法的各个指标参数。

从表1可以看出，区域一致性参数基本相同，表明3种方法分割得到的区域都符合一致性要求。本文方法的区域对比度参数略小于Mean Shift方法和渐进三角网算法，表明本文方法的分割结果在区域对比度方面略逊于后两种方法。而从模糊熵以及区域形状测度两个参数可以发现，本文方法计算的结果明显优于Mean Shift方法和渐进三角网算法。因此综合分割结果质量评价因子，本文方法更优于Mean Shift方法和渐进三角网算法。

表1 分割结果质量评价表

方法和参数		区域一致性（*UN*）	区域对比度（*GC*）	模糊熵（*E*）	区域形状测度（*SM*）	综合评价（*F*）
本文方法	*n*=1	0.978	0.188	0.733	4.158	0.552
	n=2	0.979	0.191	0.725	3.503	0.476
Mean Shift法	*bandwidth*=0.20	0.975	0.308	0.464	0.148	0.021
	bandwidth=0.15	0.979	0.289	0.449	0.192	0.024
渐进三角网加密法	—	0.979	0.306	0.505	0.002	0.0004

表2 第1套数据分割结果精度统计

计算方法	参数	地形点	
		误分率/%	漏分率/%
本文方法	*n*=1	0.95	1.39
	n=2	0.83	2.10
Mean Shift法	*bandwidth*=0.20	0.00	8.69
	bandwidth=0.15	0.16	6.11
渐进三角网加密法	—	17.37	19.65

4.3.3 精度分析

对实验原始数据进行影像辅助的人工分割，将分割结果作为真实地形，并统计地物点在本文方法、基于Mean Shift算法的分割方法、渐进三角网加密算法的分割精度情况。

从表2可以看出，从分割的准确性考察，本文方法和Mean Shift法都可以达到较好的精度，其误分率都在1%以内。而从分割的完整性考察，本文方法的漏分率明显低于Mean Shift法和渐进三角网加密方法，表明本文方法的分割完整性优于其他两种方法。

从表3也可以看出，本文方法的误分率和漏分率较低。适合作为常用方法用于点云分割过程。

表3 第2套数据分割精度统计

计算方法	参数	地形点	
		误分率/%	漏分率/%
本文方法	*n*=1	0.11	1.42

4.3.4 计算效率分析

在CPU为Intel P4 2.8 GHZ，4 G内存，Matlab2008A的软件环境中，运行本文算法和Mean Shift分割算法，在MicroStation环境下执行渐进三角网加密算法，分别记录运算时间，结果如表4所示。

从表中可以看出，同样在Matlab环境下运行，本文方法的执行效率明显优于Mean Shift法，略快于渐进三角网加密算法的执行效率。

表4 不同算法计算时间统计

计算方法	参数	计算时间/s
本文方法	*n*=1	4.7
	n=2	5.5
Mean Shift法	*bandwidth*=0.20	26.8
	bandwidth=0.15	53.2
渐进三角网加密法	—	5.5

4.4 稳定性分析

稳定性分析采用对本文方法两次计算结果的对比进行。从图5以及图6可发现，两次分割的结果基本一致。对两次分割结果中最主要区域点数进行统计，得到结果如表5所示。表中的变化率指同一区域的前一次分割点数与后一次分割点数的变化率。

从图5、图6和表5中看出，当参数选*n*=1，*cellsize*=0.55时的第8区域，在参数选*n*=2，*cellsize*=0.35时被分为第8和12区域，其余区域基本相同。

从表5中还可得知，两次分割结果中，除第6区域(3.3%)外，每一类的变化率都在1%左右，说明本文方法分割的结果具有良好的稳定性，采用不同参数计算的分割结果基本保持一致。同时，表明本文介绍的模型参数选取方法(式(5))是有效的。

表5 分割结果统计

参数	*n*=1	参数	*n*=2	变化率/%
序号	点数	序号	点数	
1	45514	1	44910	1.3
2	13690	2	13622	0.5
3	12335	3	12214	0.1
4	12137	4	12063	0.6
5	5937	5	5937	0.0
6	3302	6	3193	3.3
7	2609	7	2608	0.0
8	3193	8	2342	1.4
		12	807	
9	2141	9	2141	0.0
10	1580	10	1563	1.1
11	1211	11	1211	0.0

5 结 论

针对目前点云分割方法存在的问题，本文提出基于三维数学形态学的点云数据分割方法。采用对点云三维数字图像进行膨胀运算和聚类分析方法，完成点云分割。本文方法的关键在于确定合适的采样间隔和形态学运算次数，可通过对点云数据或航线设计数据分析，得到理想的采样间隔和形态学运算次数。通过本文方法与基于Mean Shift算法、渐进三角网加密算法分割结果的比较，可以得出结论，本文方法得到的分割结果在整体性、分割精度、计算效率、稳定性等方面优于Mean Shift算法和渐进三角网加密算法，可作为常用方法应用于点云数据分割。

本文方法的主要缺点在于无法正确分割位置相连、高程相近的不同类别点云数据。如示例数据中的建筑物和周围的树木。事实上，这也是基于点云空间数据分割方法共同的缺点。对于此类数据，还需借助其他信息，如影像光谱辅助等，才能得到较好的分割结果。

REFERENCES

Elmqvist M. 2001. Ground estimation of laser radar data using active shape models. *Proceedings*, *OEEPE Workshop on Airborne Laser Scanning and Interferometric SAR for Detailed Digital Elevation Models*, Stockholm, Sweden, Vol. XXXX

Haala N, Brenner C and Stätter C. 1998. An integrated system for urban model generation. *International Archives of Photogrammetry and Remote Sensing*, (2): 77–84

He X H, Zhou Y Y, Wang J Y, Zhou H. 2006 Image Processing Using Matlab 7.x. Beijing: The People's Posts and Telecommunications Press

Hou G X, Bi D Y and Wu C K. 2000. Researches on evaluation methods for image segmentation. *Journal of Image and Graphics*, **5**(1): 39–43

Hug C and Wehr A. 1997. Detecting and identifying topographic objects in imaging laser altimetry data. *International Archives of Photogrammetry and Remote Sensing*, **32**(3-4W2): 19–26

Kilian J, Haala N and Englich M. 1996. Capturing and evaluation of airborne laser scanner data. *International Archives of Photogrammetry and Remote Sensing, Vienna*, **32**(B3): 383–388

Kraus K and Pfeifer N. 1998. Determination of terrain models in wooded areas with ALS data. *ISPRS Journal of Photogrammetry and Remote Sensing*, **53**(4): 193–203 DOI: 10.1016/S0924-2716(98)00009-4

Kraus K and Pfeifer N. 2001. Advanced DTM generation from LIDAR data. *International Archives of Photogrammetry and Remote Sensing*, **XXXIV**(3/W4): 23–30

Li H, Li D R, Huang X F and Zhong C. 2009. Advanced adaptive TIN filter for LIDAR point clouds data. *Science of Surveying and Mapping*, **34**(3): 39–40

Liu C and Zhang Y L. 2009. Extraction of 3d feature from lidar data fused with aerial images using improved mean-shift algorithm. *International conference on Geo-spatial Solutions for Emergency Management and the 50th Anniversity of the Chinese Academy of Surveying and Mapping*, *Beijing*, *China,* **XXXVIII**(Part 7-C4): 20–24

Liu J N and Zhang X H. 2005. Classification of laser scanning altimetry data using laser intensity. *Geomatics and Information Science of Wuhan University*, **30**(3): 189–193

Lohmann P, Koch A and Schaeffer M. 2000. Approaches to the filtering of laser scanner data. *International Archives of Photogrammetry and Remote Sensing*, **33**(B3): 540–547

Roggero M. 2001. Airborne laser scanning: clustering in raw data. *International Archives of the Photogrammetry and Remote Sensing*, **34**(B3-W4): 227–232

Sithole G. 2001. Filtering of laser altimetry data using a slope adaptive filter. *International Archives of Photogrammetry and Remote Sensing*, **34**(3-W4): 203–210

Sithole G. 2005. Segmentation and Classification of Airborne Laser Scanner Data. Delft: Technical University of Delft

Vosselman G. 2000. Slope based filtering of laser altimetry data. *International Archives of Photogrammetry and Remote Sensing*, **33**(B3): 935–942

Weidner U and Forstner W. 1995. Towards automatic building extraction from high resolution digital elevation models, *ISPRS Journal of Photogrammetry and Remote Sensing*, **50**(4): 38–49

Xu J H. 2002. The Mathematical Methods in Contemporary Geography. 2nd ed. Beijing: Higher Education Press

Zhang K Q, Chen S C, Whitman D, Shyu M L, Yan J H and Zhang C C. 2003. A progressive morphological filter for removing nonground measurements from airborne LIDAR data. *IEEE Transactions on Geoscience and Remote Sensing*, **41**(4): 872–882

Zhang K Q and Whitman D. 2005. Comparison of three algorithms for filtering airborne LIDAR data. *Photogrammetric Engineering and Remote Sensing*, **71**(3): 313–324

附中文参考文献

侯格贤，毕笃彦，吴成柯．2000．图象分割质量评价方法研究．中国图象图形学报，**5**(1): 39–43

贺兴华，周媛媛，王继阳，周晖．2006．MatLab 7.x图像处理．北京: 人民邮电出版社

李卉，李德仁，黄先锋，钟成．2009．一种渐进加密三角网LIDAR点云滤波的改进算法．测绘科学，**34**(3): 39–40

刘经南，张小红．2005．利用激光强度信息分类激光扫描测高数据．武汉大学学报(信息科学版)，**30**(3): 189–193

徐建华．2002．现代地理学中的数学方法(第二版)．北京: 高等教育出版社